Constructive Lyapunov Control Design for Turbocharged Diesel Engines

Mrdjan Jankovic, *Senior Member, IEEE*, Miroslava Jankovic, and Ilya Kolmanovsky, *Member, IEEE*

***Abstract*—This paper presents a control design method for diesel engines equipped with a variable geometry turbocharger and an exhaust gas recirculation valve. Our control objective is to regulate the air-fuel ratio and the fraction of recirculated exhaust gas to their respective set points that depend on engine operating conditions. Interactions between the two actuators and nonlinear behavior of the system make the problem difficult to handle using classical control design methods. Instead, we employ a recently developed control Lyapunov function (CLF) based nonlinear control design method because it possesses a guaranteed robustness property equivalent to gain and phase margins. The CLF is constructed using input–output linearization of a reduced order diesel engine model. The controller has been tested in simulations on the full order model as well as experimentally in the dynamometer test cell.**

***Index Terms*—Diesel engines, Lyapunov methods, nonlinear control, turbocharging.**

NOMENCLATURE

AF	Air-fuel ratio.
N	Engine speed.
p_1	Intake manifold pressure.
p_2	Exhaust manifold pressure.
p_a	Ambient pressure.
T_1	Intake manifold temperature.
T_2	Exhaust manifold temperature.
T_e	Temperature of the exhaust gas from the engine.
T_c	Temperature of air at the compressor outlet.
T_{egr}	Temperature of recirculated gas entering the intake manifold.
m_1	Mass of gas in the intake manifold.
m_2	Mass of gas in the exhaust manifold.
F_1	Fraction of burned gas in the intake manifold.
F_2	Fraction of burned gas in the exhaust manifold.
V_1	Volume of the intake manifold.
V_2	Volume of the exhaust manifold.
P_c	Compressor power.
P_t	Turbine power.
ω_{tc}	Turbocharger speed.
J_{tc}	Turbocharger moment of inertia.
W_f	Engine fueling rate requested by the driver.
W_c	Compressor air mass flow rate.
W_t	Turbine gas mass flow rate.
W_e	Total mass flow rate into the engine.
W_{egr}	EGR mass flow rate.
EGR	EGR flow fraction defined as $W_{\mathrm{egr}}/(W_{\mathrm{egr}}+W_c)$.
η_c	Compressor isentropic efficiency.
η_t	Turbine isentropic efficiency.
η_m	Turbocharger mechanical efficiency.
c_p, c_v	Specific heat at constant pressure, volume, respectively.
γ	Specific heat ratio c_p/c_v (1.4 for air).
R	Specific gas constant equal to $c_p - c_v$.

Manuscript received March 3, 1998; revised March 9, 1999. Recommended by Associate Editor, F. Ghorbel.

The authors are with Ford Research Laboratory, Dearborn, MI 48121 USA (e-mail: mjankov1@ford.com).

Publisher Item Identifier S 1063-6536(00)01416-0.

I. INTRODUCTION

A NUMBER of theoretical advances in recent years (cf. [5], [9], [16], [17], and [22]) have brought the understanding of nonlinear control systems to a level where it can be used to solve practical control design problems. Still, much more effort is needed for the tools and techniques of nonlinear control to become a well-established approach to control design. A part of this effort is to develop guidelines and patterns for application of nonlinear control to practical problems. In this paper we propose a controller for a nonlinear, multivariable turbocharged diesel engine model. Besides providing one solution to a difficult and important design problem, we hope that this paper would also serve as an illustration of how to apply control Lyapunov function-based techniques to problems of practical interest.

The basic performance requirements for automotive engines in terms of peak power, transient response, fuel economy, and emissions are often contradictory and require judicious tradeoff's at every stage of the design process. Diesel (compression ignition) engines hold a significant advantage over spark ignited (gasoline) engines in fuel economy. Moreover, diesel engines have lower feed-gas emissions of the regulated exhaust gases, but the after-treatment devices for diesel engines are far less efficient than the conventional three way catalysts for spark ignition engines. A particular problem is a high level of oxides of nitrogen NO and NO_2 (in short NO_x) in the tail-pipe emissions of diesel engines. A very effective way to reduce the formation of NO_x during combustion is to recirculate the exhaust gas through the exhaust gas recirculation (EGR) valve into the intake manifold. Presence of the inert exhaust gas in the cylinder reduces peak temperature of combustion and suppresses formation of NO_x. The fraction of EGR recirculated into the intake manifold must be scheduled on the operating condition, because high EGR levels reduce the amount of fresh air and cannot be maintained at high loads.

To improve its relatively low power density, a diesel engine can be equipped with a turbocharger which consists of a turbine and a compressor attached to the same shaft. A portion of the energy of the exhaust gas is transferred by the turbine to the compressor to increase the pressure in the intake manifold. Design of a conventional turbocharger faces a tradeoff between fast transient response at low engine speeds and high engine power output without turbine overspeeding at high engine speeds [18]. This tradeoff can be alleviated by employing a variable geometry turbocharger (VGT) to control the amount of exhaust gas flowing through the turbine and the turbine power transfer by changing the position of the guide vanes.

For diesel engines equipped with the EGR and VGT actuators, the design objective is to supply an amount of air and a fraction of EGR appropriate for a given operating condition (engine speed and fueling rate demanded by the driver). An insufficient amount of air leads to an increase in particulate emissions and possibly visible smoke, while an insufficient EGR fraction leads to an increase in NO_x emissions. In addition, the system has to provide fast increase of engine air intake at driver tip-ins to allow fast increase in fueling rate and, hence, engine torque.

The nonlinear multivariable nature of the plant to be controlled and dual design objective make this control design problem difficult [4], [15]. A good solution must provide a robust controller that does not use up much resources of the electronic control unit and is simple to implement and calibrate. In this paper we employ a recently proposed nonlinear control design method [22] that applies to multivariable systems and achieves robustness of optimal controllers (nonlinear equivalent of $(1/2, \infty)$ gain margin and $\pm$ 60° phase margin). Starting from a control Lyapunov function (CLF), the robustness is achieved by the *domination redesign* [11], [22]. A CLF is constructed for a simplified model by employing input–output linearization, a tool of geometric control theory. Input–output linearization also provides a stabilizing control law, but the cancellations associated with it may result in increased complexity and sensitivity. In contrast, the robustness property guaranteed by the domination redesign method is an indicator of low sensitivity of the closed-loop system to unmodeled dynamics and parametric uncertainties.

In the Section II we review the basic properties and present a standard model of a turbocharged diesel engine. The engine is modeled as a series of control volumes interconnected via orifices of varying geometry. The dynamical model is developed using the conservation of energy and mass together with several experimentally derived maps (turbine and compressor efficiencies, engine pumping, etc.). The result is the seventh-order model of the turbocharged diesel engine to which one can add the dynamics of the two actuators. In Section III we review the domination redesign method as a tool for designing controllers that achieve robustness of optimal systems. The basic assumption is that a CLF is available. Constructing a CLF may be a difficult task, in particular, if simplicity of the control law generated by the domination redesign is one of the design objectives. With this in mind, in Section IV we propose a simplified third-order model of the engine. The controller design then proceeds through a sequence of steps: selection of outputs which are minimum phase, input–output linearization, construction of a CLF, and domination redesign. Finally, in Section V we show how the nonlinear controller performed in simulations on the full-order turbocharged diesel engine model as well as experimentally in a dynamometer test cell.

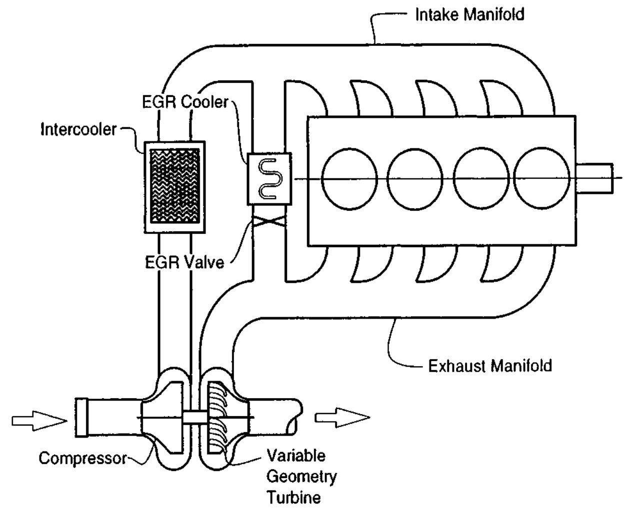

Fig. 1. Turbocharged diesel engine.

II. Modeling of Turbocharged Diesel Engines

In this section we present a model of a diesel engine equipped with a variable geometry turbocharger and an exhaust gas recirculation valve based on the mean-value diesel engine models reported in [2], [12], [14], [15], [26], and [27]. The presentation, which closely follows [15], [26], serves the purpose of establishing basic physical properties of a turbocharged diesel engine that play a role in the controller design.

The schematic diagram of a diesel engine is shown in Fig. 1. At the bottom of the diagram is the turbocharger consisting of a variable geometry turbine and a compressor mounted on the same shaft. The turbine takes the energy from the exhaust gas to power the compressor. The mixture of air from the compressor and exhaust gas coming through the EGR valve is pumped from the intake manifold into the cylinders. The fuel is injected directly into the cylinders and burned, producing the torque on the crank shaft. The hot exhaust gas is pumped out into the exhaust manifold. Part of the exhaust gas flows from the exhaust manifold through the turbine out of the engine and the other part is recirculated back into the intake manifold. The diagram also shows the intercooler and the EGR-cooler that are used to reduce the intake manifold temperature. For the sake of simplicity we have not included the coolers in the model.

The mean value diesel engine model is based on the conservation of mass and energy and the ideal gas law. According to the mass conservation law, the change of mass in the volume is equal to the difference of the flows into and out of the volume. Hence, the change of masses of gas in the intake and exhaust manifolds are

$$\dot{m}_1 = W_c + W_{\mathrm{egr}} - W_e \tag{2.1}$$

$$\dot{m}_2 = W_e - W_{\mathrm{egr}} - W_t + W_f. \tag{2.2}$$

The first law of thermodynamics (conservation of energy) gives us two more equations that govern the change of pressures in the intake and exhaust manifolds, respectively:

$$\dot{p}_1 = \frac{\gamma R}{V_1}(W_c T_c + W_{\mathrm{egr}} T_{\mathrm{egr}} - W_e T_1) \tag{2.3}$$

$$\dot{p}_2 = \frac{\gamma R}{V_2}((W_e + W_f)T_e - W_{\mathrm{egr}}T_2 - W_t T_2) \tag{2.4}$$

where the heat transfer to the surroundings has been neglected. The temperatures of gas in the intake and exhaust manifolds are then computed from the ideal gas law

$$p_i V_i = m_i R T_i, \qquad i = 1, 2. \tag{2.5}$$

The temperature of the exhaust from the engine is given by $T_e = T_1 + T_r$ where the temperature rise T_r can be modeled based on the static engine data as a function of the fuel flow, air-fuel ratio, and the fraction of burned gas in the intake manifold, F_1.

The flow through the EGR valve is modeled by the standard orifice flow equation

$$W_{\mathrm{egr}} = \begin{cases} C_{\mathrm{egr}}(\kappa_{\mathrm{egr}})\dfrac{p_2}{\sqrt{RT_2}}\,\Psi\left(\dfrac{p_1}{p_2}\right) & \text{if } p_1 < p_2 \\ 0 & \text{if } p_1 = p_2 \\ C_{\mathrm{egr}}(\kappa_{\mathrm{egr}})\dfrac{p_1}{\sqrt{RT_1}}\,\Psi\left(\dfrac{p_2}{p_1}\right) & \text{if } p_1 > p_2 \end{cases} \tag{2.6}$$

where C_{egr} is the effective flow area of the EGR valve expressed as a function of the normalized EGR valve opening $\kappa_{\mathrm{egr}} \in [0, 1]$ and where the pressure ratio correction factor is given by

$$\Psi\left(\frac{p_i}{p_j}\right) = \begin{cases} \gamma^{1/2}\left(\dfrac{2}{\gamma+1}\right)^{((\gamma+1)/2(\gamma-1))} \\ \text{if } \dfrac{p_i}{p_j} \le \left(\dfrac{2}{\gamma+1}\right)^{\gamma/(\gamma-1)} \\ \sqrt{\dfrac{2\gamma}{\gamma-1}\left(\left(\dfrac{p_i}{p_j}\right)^{2/\gamma} - \left(\dfrac{p_i}{p_j}\right)^{(\gamma+1)/\gamma}\right)} \\ \text{if } \dfrac{p_i}{p_j} > \left(\dfrac{2}{\gamma+1}\right)^{\gamma/\gamma-1}. \end{cases} \tag{2.7}$$

A modified version of the orifice flow equation adopted from [15] is used to model the turbine flow W_t

$$W_t = C_{\mathrm{vgt}}(\kappa_{\mathrm{vgt}})\frac{p_2}{\sqrt{RT_2}}\,\Psi_2\left(\frac{p_a}{p_2}, \kappa_{\mathrm{vgt}}\right). \tag{2.8}$$

Both the effective flow area C_{vgt} of the turbine, and the pressure ratio correction factor Ψ_2 depend on the normalized opening of the variable geometry turbocharger $\kappa_{\mathrm{vgt}} \in [0, 1]$.

The engine pumping rate is a linear function of the intake manifold pressure with the coefficient of proportionality k_e dependent on engine speed and intake manifold temperature

$$W_e = k_e(N, T_1)p_1. \tag{2.9}$$

The engine pumping coefficient can be obtained from the static engine data. It weakly depends on the exhaust pressure and the cylinder wall temperature, but these dependencies are neglected in this development.

As a result of lean combustion (the mixture in the cylinder contains more air than the stoichiometric[1] one) the exhaust from the engine is not entirely burned gas (i.e., contains extra air) and so does the gas being recirculated into the intake manifold through the EGR valve. The dynamics of fractions of burned gas in the intake manifold F_1 and exhaust manifold F_2 is derived in [15] as

$$\dot{F}_1 = \frac{W_{\mathrm{egr}}(F_2 - F_1) - W_c F_1}{m_1} \tag{2.10}$$

$$\dot{F}_2 = \frac{W_e[15.6(1-F_1) + (\mathrm{AF}+1)\,F_1]/(\mathrm{AF}+1) - W_e F_2}{m_2}. \tag{2.11}$$

The state equation for the turbocharger speed is derived from the Newton's second law with the turbine and compressor torques represented as the ratios of their respective powers and the turbocharger speed

$$\dot{\omega}_{tc} = \frac{1}{J_{tc}\omega_{tc}}(\eta_m P_t - P_c). \tag{2.12}$$

The expression for turbine power P_t can be derived following [24]. Using the simplified version of the steady flow equation, under the assumption that the process is isentropic, we obtain an expression for the turbine power as $P_t = W_t \Delta h = W_t c_p (T_2 - T_s)$ where

Δh difference between inlet and outlet enthalpies;
T_s temperature at the outlet of an isentropic turbine.

From the pressure ratio across the turbine, an isentropic temperature ratio can be found

$$\frac{T_s}{T_2} = \left(\frac{p_a}{p_2}\right)^{\mu}, \qquad \mu := \frac{\gamma-1}{\gamma} = 0.285. \tag{2.13}$$

For a real turbine, the power is given by

$$P_t = W_t \Delta h = W_t c_p (T_2 - T_b) \tag{2.14}$$

where T_b is the turbine outlet temperature which is different from T_s. We account for heat losses by introducing turbine isentropic efficiency

$$\eta_t = \frac{T_2 - T_b}{T_2 - T_s}. \tag{2.15}$$

In general, turbine isentropic efficiency η_t depends on VGT opening, pressure ratio across the turbine, and turbocharger speed.

Substituting (2.13) and (2.15) into (2.14) we obtain the expression for the turbine power in terms of the pressure ratio across the turbine

$$P_t = W_t c_p \eta_t T_2 \left[1 - \left(\frac{p_a}{p_2}\right)^{\mu}\right]. \tag{2.16}$$

[1]The mixture is stoichiometric if it contains chemically exact mass of air to burn all the fuel injected. For diesel fuel the stoichiometric air–fuel ratio is around 14.6.

Following the same approach one can derive the expression for the compressor power

$$P_c = W_c c_p \frac{1}{\eta_c} T_a \left[\left(\frac{p_1}{p_a} \right)^{\mu} - 1 \right]. \tag{2.17}$$

The temperature of air at the compressor outlet can be expressed as

$$T_c = T_a \left[1 + \frac{1}{\eta_c} \left(\left(\frac{p_1}{p_a} \right)^{\mu} - 1 \right) \right]. \tag{2.18}$$

In contrast to the turbine mass flow rate which is obtained from the orifice flow equation, the compressor mass flow rate W_c is determined from the compressor characteristic supplied by the manufacturer as a function of the pressure ratio and turbocharger speed: $W_c = W_c((p_1/p_a), \omega_{tc})$. The same can be done to determine the compressor isentropic efficiency η_c.

The gas coefficients c_p, c_v, γ, and R are weak functions of the gas composition, that is F_1 and F_2, and temperature. This dependence is typically neglected and the coefficients are treated as constants. The only remaining variable which weakly depends on the gas composition states F_1 and F_2 is the exhaust temperature T_2, rendering F_1 and F_2 almost unobservable from the other five states. Nevertheless, the composition states are important because F_1 significantly affects one of the performance measures, emissions of NO_x.

Finally, we must emphasize that the model of a turbocharged diesel engine presented in this section is not used for controller design. Rather, its augmented version is employed to verify the performance of the controller in simulations.

III. Robust Nonlinear Control Design

The controller to be designed must achieve desired performance in spite of a significant level of uncertainties present in a turbocharged diesel engine. The sources of uncertainty include parametric uncertainty due to engine-to-engine variability and aging, uncertainties in turbine and compressor models, heat losses, unmodeled actuator dynamics, and variations in the ambient conditions. To cope with uncertainty in the model, we use a recently developed control design method [11], [22] which applies to nonlinear multivariable systems and guarantees robustness of optimal controllers. This method is briefly reviewed next.

A. Robustness to Input Unmodeled Dynamics

The success of the classical frequency domain design methods in practice is in part due to the fact that they give the designer control over important indicators of robustness of the feedback system: the gain and phase margins. Full state linear optimal controllers, called linear quadratic regulators (LQR's), are also known for their robustness which has been interpreted as $(1/2, \infty)$ gain margin and $\pm 60°$ phase margin [1]. From the connection between optimality and passivity established by Kalman [13], one can also interpret this robustness property as a stability guarantee in the presence of input unmodeled dynamics satisfying a dissipativity property. The same robustness

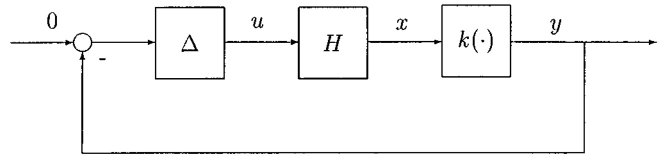

Fig. 2. Nonlinear feedback loop with the control law $k(x)$ and an input uncertainty Δ.

property holds for nonlinear optimal systems [6], [25], because the connection between optimality and passivity extends to nonlinear systems [19], [20].

The input uncertainty Δ which perturbs the nominal feedback system consisting of the nominal plant H

$$H: \dot{x} = f(x) + g(x)u \tag{3.1}$$

and the nominal feedback law $u = -k(x)$, as depicted in Fig. 2, is assumed to satisfy the following properties.

1) The uncertainty Δ is of the form

$$\dot{\zeta} = f(\zeta, u_\Delta)$$
$$y_\Delta = h(\zeta, u_\Delta)$$

where u_Δ and y_Δ are the input and the output of Δ and, when $u_\Delta \equiv 0$, Δ is globally asymptotically stable.

2) For some $\nu > 1/2$, the system $\Delta - \nu I$ is passive. In other words, there exists a positive semidefinite, radially unbounded function $W_\Delta(\zeta)$ such that

$$\dot{W}_\Delta \le y_\Delta^T u_\Delta - \nu u_\Delta^T u_\Delta. \tag{3.2}$$

The condition $\nu > (1/2)$ has been chosen because it provides a connection with optimality. Robustness to Δ satisfying (3.2) for any $\nu > \varepsilon > 0$ can also be achieved by rescaling the control [22]. The class of uncertainties Δ that satisfy the above conditions is denoted by $\mathcal{I}$. This class of uncertainties includes static gains $\mathrm{diag}\{\kappa_i\}$ with $\kappa_i \in (1/2, \infty)$ (hence $(1/2, \infty)$ gain margin); sector nonlinearities[2] $\mathrm{diag}\{\varphi_i(\cdot)\}$ with $\varphi \in (1/2, \infty)$; stable linear systems that satisfy $\mathrm{Re}\{G(j\omega)\} > 1/2$ (this implies $\pm 60°$ phase margin); a wide class of nonlinear systems including many for which no input–output gain can be defined [22].

The class of systems $\mathcal{I}$ includes only the dynamical systems with relative degree 0. In the linear case such uncertainties arise when a pole-zero pair is neglected; for example, when weakly observable or weakly controllable dynamics are neglected. Also, parametric uncertainties can be represented by an uncertainty with relative degree 0[22].

The robustness to uncertainties Δ in $\mathcal{I}$ is closely connected to optimality of the control law $u = -k(x)$. Indeed, LQR feedback systems are robust to all Δ in $\mathcal{I}$. Conversely, if a linear control law is not LQ optimal, then there exists an uncertainty Δ in $\mathcal{I}$ such that the perturbed system is unstable [22].

[2]A nonlinear function $\varphi(\cdot)$ is said to belong to a sector (a, b), denoted by $\varphi \in (a, b)$, if $as^2 < s\varphi(s) < bs^2$.

Similarly, in the nonlinear case, the perturbed feedback loop remains stable for all Δ in $\mathcal{I}$ provided that the control law $u = -k(x)$ is optimal for some cost of the form

$$J = \int_0^\infty l(x) + u^T u \, dt, \qquad l(x) \geq 0. \tag{3.3}$$

The robustness of optimal control follows from the Hamilton–Jacobi–Bellman (HJB) partial differential equation satisfied by the optimal value function $V(x)$. For the cost (3.3) the HJB equation is given by

$$l(x) + L_f V(x) - \tfrac{1}{4} L_g V(x)(L_g V)^T(x) = 0 \tag{3.4}$$

and the optimal control law is

$$u(x) = -\tfrac{1}{2} (L_g V)^T(x). \tag{3.5}$$

The notation $L_p h(x)$ denotes the Lie derivative of a function $h(x)$ along a vector field $p(x)$: $L_p h(x) := (\partial h/\partial x) p(x)$.

Thus, one method to achieve robustness to uncertainties in $\mathcal{I}$ is to set up an optimal control problem and find the optimal control law. In general, this approach is not feasible because it is very difficult to solve the HJB equation. Instead, because any optimal control law for a cost of the form (3.3) possesses the desired robustness property, we try to achieve *inverse optimality* in which some *a priori* choice of the control Lyapunov function determines the cost functional and the optimal control law.

B. Inverse Optimal Control Design

The starting point for our inverse optimal design for the nonlinear system H (3.1) is the knowledge of a *control Lyapunov function* (CLF) [3], a smooth, positive definite, radially unbounded function $V(x)$ which satisfies that for all $x \neq 0$ there exists u such that

$$\dot{V}(x) = L_f V(x) + L_g V(x) u < 0. \tag{3.6}$$

Note that (3.6) is equivalent to $L_g V(x) = 0 \Rightarrow L_f V(x) < 0$ for $x \neq 0$.

Starting from a CLF, several control laws have been proposed in the literature (cf. [5], [23]). These control laws are smooth everywhere except at the origin, continuous at the origin (under a mild additional assumption), and robust to static uncertainties in $\mathcal{I}$. A stronger robustness property can be guaranteed by applying the *domination redesign* [22] briefly reviewed here.

Define a *dominating function* γ: $\mathbb{R}^+ \to \mathbb{R}^+$ to satisfy

$$\gamma(V(x)) \geq 2 p_S(x), \qquad \forall\, x \in \mathbb{R}^n \tag{3.7}$$

$$\lim_{t \to \infty} \int_0^t \gamma(s)\, ds = +\infty \tag{3.8}$$

where

$$p_S(x) := \begin{cases} \dfrac{L_f V + \sqrt{(L_f V)^2 + \|L_g V\|^4}}{\|L_g V\|^2} & \text{if } \|L_g V(x)\| \neq 0 \\ 0 & \text{if } \|L_g V(x)\| = 0. \end{cases} \tag{3.9}$$

If $p_S(x)$, which is nonnegative for all $x \in \mathbb{R}^n$, is bounded on compact sets, a dominating function $\gamma(\cdot)$ always exists.

It turns out that

$$\tilde{V}(x) := \int_0^{V(x)} \gamma(s)\, ds$$

is a smooth, positive definite, and radially unbounded optimal value function for a cost of the form (3.3). The optimal control law obtained by the domination redesign is given by

$$u(x) = -\tfrac{1}{2}(L_g \tilde{V})^T(x) = -\tfrac{1}{2}\gamma(V(x))(L_g V(x))^T. \tag{3.10}$$

If the function $p_S(x)$ in not bounded on compact sets (cf. the system $\dot{x} = x^2 + xu$) the domination redesign does not apply. In [11] the following sufficient condition for boundedness of $p_S(x)$ on compact sets is given.

- The quadratic part V_2 of the CLF V [$V_2 := (1/2)x^T(\partial^2 V/\partial x^2)(0)x$] is a CLF for the Jacobian linearization at the origin of the nonlinear system (3.1).

This sufficient condition implies that the Jacobian linearization of the nonlinear system (3.1) is stabilizable. For systems with nonstabilizable Jacobian linearization applicability of the domination redesign may depend on the choice of a CLF [11].

The control law can be simplified by choosing $\gamma(V(x)) = \gamma_0$, with $\gamma_0 > 0$ constant. The global stability is lost, but optimality and asymptotic stability with any desired region of attraction can be achieved by selecting γ_0 sufficiently large. This can be established as follows. Because V is radially unbounded, for any desired region of attraction $U \subset \mathbb{R}^n$, we can always find a constant c such that $L := \{x \in \mathbb{R}^n\colon V(x) \leq c\} \supset U$ is a compact set. Choose γ_0 to satisfy

$$\gamma_0 > 2 \sup_{x \in L} p_S(x). \tag{3.11}$$

Then $u = -(1/2)\gamma_0 (L_g V(x))^T$, resulting in

$$\dot{V} = L_f V - \tfrac{1}{2}\gamma_0 \|L_g V\|^2 \leq -\sqrt{(L_f V)^2 + \|L_g V\|^4} < 0$$

for all $x \in L$, $x \neq 0$, achieves asymptotic stability with the region of attraction containing U. Optimality follows because $\tilde{V} = \gamma_0 V$ satisfies an HJB equation

$$\tilde{l}(x) + L_f \tilde{V} - \tfrac{1}{4}\|L_g \tilde{V}\|^2 = 0$$

with $\tilde{l}(x)$ defined by $\tilde{l}(x) := -L_f \tilde{V} + (1/4)\|L_g \tilde{V}\|^2 \geq \gamma_0 (L_f V - \sqrt{(L_f V)^2 + \|L_g V\|^4}) \geq 0$.

C. Stabilizing Control and CLF

The domination redesign control law requires that a CLF be known. In most cases, construction of a CLF cannot be separated from a design of a stabilizing control law. A Lyapunov function that is used to establish stability of the closed-loop system becomes a CLF for the open-loop system. Given this connection between a CLF and a stabilizing feedback law, the question is why are we interested in the domination redesign?

In many cases, construction of a stabilizing control involves cancellation of terms in the system dynamics. The design is often greatly simplified if we rely on exact cancellation of nonlinearities or interconnection terms between subsystems. However, in practice, such cancellations may not be feasible due to uncertainties and actuator saturation. In addition, cancelling a term that may have stabilizing effect results in positive feedback, increased sensitivity, and wasted control effort.

The main advantage of the domination redesign is that we are able to replace a control law obtained in the process of constructing a CLF with an inverse optimal one that possesses gain and phase margins. In view of this, we are not at all concerned by the cancellations we employ in constructing the initial stabilizing control law. At this stage our objective is to generate a Lyapunov function (CLF) with some desired properties. For example, in the control design presented in the next section, domination redesign control law is simpler than the original input–output linearizing one because the CLF we constructed is simple.

It is desirable that the Lyapunov function (that is the CLF) be parameterized by parameters that become adjustable feedback gains in the domination redesign control law. Several control design methods which may be used in the initial stage, such as feedback linearization [9], backstepping [16], and forwarding [22], allow construction of such parameterized Lyapunov functions. Additional degrees of freedom for a multiinput system can be obtained by having different gains in different input channels. The feedback law

$$u = -\tfrac{1}{2}\,\Gamma (L_g V)^T(x), \qquad \Gamma := \mathrm{diag}\{\gamma_1, \cdots, \gamma_m\}$$

guarantees asymptotic stability (in L) and optimality if $\gamma_i \geq \gamma_0$ with γ_0 defined in (3.11). The above guidelines are followed in the next section in designing a controller for the diesel engine.

IV. Controller Design for Turbocharged Diesel Engine

Let us now return to the turbocharged diesel control design problem. The design objectives are the following.

1) Regulation of the air-fuel ratio and EGR fraction to their respective set points determined by the operating conditions during quasi steady state operation (i.e., cruising, slow acceleration or deceleration);
2) Fast increase in engine air intake at driver tip-in;
3) Graceful degradation in performance if the set points are not feasible;
4) Simplicity of the control law is highly desirable for implementation.

The design objectives are used as guidelines in the controller design, including the selection of the control oriented model. Complexity of the model affects the control law, so we have decided to simplify the seventh-order model described in Section II.

First we remove the states F_1 and F_2 from the model even though F_1, the fraction of burned gas in the intake manifold, is a performance variable. The two states are difficult to measure and are only weakly observable from the other five states. The steady state value of F_1 will be regulated by regulating the AF ratio and EGR flow fraction.

Next we remove the states m_1 and m_2 from the model. Our motivation is that these states are relatively difficult to control separately from p_1 and p_2, in particular if the intercooler and the EGR-cooler are present. In the reduced order model given below, the differential equations for p_1 and p_2 are derived from the ideal gas law and T_1 and T_2 are treated as external, slowly varying signals. Such an approach is well established for modeling intake manifolds in spark-ignited engines [7], [8]. As an additional simplification, the turbocharger dynamics is modeled as a first-order lag power transfer with time constant τ

$$\begin{aligned}\dot{p}_1 &= k_1(W_c + W_{\mathrm{egr}} - k_e p_1) + \frac{\dot{T}_1}{T_1}\,p_1\\ \dot{p}_2 &= k_2(k_e p_1 - W_{\mathrm{egr}} - W_t + W_f) + \frac{\dot{T}_2}{T_2}\,p_2\\ \dot{P}_c &= \frac{1}{\tau}(\eta_m P_t - P_c)\end{aligned} \tag{4.1}$$

where $k_i := (RT_i/V_i)$, $i = 1, 2$. As it is standard in modeling the intake manifolds in spark-ignited engines, we neglect the temperature derivatives in (4.1). Temperature sensors used for engine control have time constants in the order of seconds and, hence, are not fast enough to provide usable $\dot{T}_1$ and $\dot{T}_2$ signals. Moreover, steady-state values are not affected by the two terms.

To simplify the controller design we assign the roles of the control inputs to the flows W_{egr} and W_t denoted by v_1 and v_2, respectively. An implicit assumption in doing this is that the desired flow values can be assigned by manipulating the EGR and VGT actuators. The maps from the actuator openings κ_{egr} and κ_{vgt} can be inverted, but we should keep in mind that both actuators are subject to saturation creating, in effect, state dependent saturations for v_1 and v_2. Hence, our control design model becomes

$$\begin{aligned}\dot{p}_1 &= k_1(W_c + v_1 - k_e p_1)\\ \dot{p}_2 &= k_2(k_e p_1 - v_1 - v_2 + W_f)\\ \dot{P}_c &= \frac{1}{\tau}(\eta_m P_t - P_c)\end{aligned} \tag{4.2}$$

with the nonlinearities contained inside the functions

$$W_c = \frac{\eta_c}{T_a c_p}\,\frac{P_c}{p_1^{\mu} - 1}, \qquad P_t = \eta_t c_p T_2\left(1 - \frac{1}{p_2^{\mu}}\right) v_2. \tag{4.3}$$

For the sake of simplicity we have assumed that $p_a = 1$ (bar), and it has been dropped from the expressions for W_c and P_t [cf. (2.16) and (2.17)].

The diesel engine model has a singularity at $p_1 = 1$ when the compressor flow becomes infinite. Fortunately, it can be shown that the set $\Omega := \{(p_1, p_2, P_c){:}\, p_1 > 1, p_2 > 1, P_c > 0\}$ is invariant; that is, every trajectory starting in Ω stays in Ω for all t.

A. Setting Up the Control Design Problem

Our design objective is to regulate the air-fuel ratio and the EGR flow fraction to the set points determined from the static engine data

$$\mathrm{AF}_{ref} = \mathrm{AF}_{ref}(N, W_f), \quad \mathrm{EGR}_{ref} = \mathrm{EGR}_{ref}(N, W_f). \tag{4.4}$$

Because the air-fuel ratio and EGR fraction are not measured in a vehicle, we transform their set points into the set points for the compressor and the EGR mass flow rates using their relationship in steady state, $\mathrm{AF} = (1 - F_1)(W_c + W_{\mathrm{egr}})/W_f$, and the steady state value of F_1 derived from (2.10) to obtain (4.5) shown at the bottom of the next page. Thus, the control design objective is to regulate

$$y_1 := W_c - W_c^d \quad \text{and} \quad y_2 := W_{\mathrm{egr}} - W_{\mathrm{egr}}^d \tag{4.6}$$

to zero.

To find equilibrium points of the system consistent with $y_1 = y_2 = 0$ we compute

$$\dot{y}_1 = -a(y_1 + W_c^d - k_e p_1) - \frac{1}{\tau}(y_1 + W_c^d) - av_1 + bv_2 \quad (4.7)$$

where

$$a := k_1 \frac{\mu p_1^{\mu-1}(y_1 + W_c^d)}{p_1^\mu - 1}, \qquad b := \frac{1}{\tau}\,\eta^* \frac{T_2}{T_a}\,\frac{1 - p_2^{-\mu}}{p_1^\mu - 1} \quad (4.8)$$

with $\eta^* := \eta_m \eta_c \eta_t$. Solving the equations $\dot{y}_1 = 0$ and $y_2 = 0$ for v_1 and v_2 we obtain

$$v_1 = W_{\mathrm{egr}}^d, \qquad v_2 = \frac{a(W_c^d + W_{\mathrm{egr}}^d - k_e p_1) - \dfrac{1}{\tau} W_c^d}{b}.$$

Substitution of these values for v_1, v_2, and $y_1 = y_2 = 0$ into the dynamics for p_1 and p_2 leads to

$$\begin{aligned}\dot{p}_1 &= k_1(-k_e p_1 + W_c^d + W_{\mathrm{egr}}^d)\\ \dot{p}_2 &= k_2\left[\frac{a+b}{b}(k_e p_1 - W_c^d - W_{\mathrm{egr}}^d) + W_c^d + W_f - \frac{1}{\tau b} W_c^d\right].\end{aligned} \quad (4.9)$$

The system (4.9) has a unique equilibrium at

$$\begin{aligned}p_{1e} &= \frac{W_c^d + W_{\mathrm{egr}}^d}{k_e}\\ p_{2e} &= \left(1 - \frac{W_c^d}{W_c^d + W_f}\,\frac{T_a}{T_2 \eta^*}(p_{1e}^\mu - 1)\right)^{-(1/\mu)}\end{aligned} \quad (4.10)$$

The equilibria for W_c and p_1 give the equilibrium value for the compressor power

$$P_{ce} = \frac{T_a c_p}{\eta_c}\, W_c^d (p_{1e}^\mu - 1).$$

Hence, there exists a unique equilibrium (p_{1e}, p_{2e}, P_{ce}) of the system (4.2) consistent with $y_1 = y_2 = 0$.

B. Construction of a CLF

Input–output linearization is a method of rendering the input–output behavior of a multivariable nonlinear system the same as that of m chains of integrators [9] (m is a dimension of the input and output vectors). This method of geometric control theory is useful for analysis and control design. We employ it here to construct a CLF for the diesel engine model.

Input–output linearization is applicable if, by differentiating each output y_i of a nonlinear system

$$\begin{aligned}\dot{x} &= f(x) + g(x)v\\ y &= h(x) + j(x)v, \qquad v, y \in \mathbb{R}^m\end{aligned} \quad (4.11)$$

r_i times, $i = 1, \cdots, m$, $\sum r_i \le n$, we can write

$$\begin{bmatrix} y_1^{(r_1)} \\ y_2^{(r_2)} \\ \vdots \\ y_m^{(r_m)} \end{bmatrix} = F(x) + G(x)v$$

with $G(x)$ being an invertible matrix. Then by applying the feedback and input transformation $v = G^{-1}(x)(u - F(x))$ and a change of coordinates $x \to (z, y_1, \cdots, y_1^{(r_1-1)}, \cdots, y_m^{(r_m-1)})$, where $z \in \mathbb{R}^l$, $l = n - r_1 - \cdots - r_m$, we can transform the system (4.11) into the form

$$\begin{aligned}y_1^{(r_1)} &= u_1\\ &\vdots\\ y_m^{(r_m)} &= u_m\\ \dot{z} &= f_0(z, y_1, \cdots, y_1^{(r_1-1)}, \cdots, y_m^{(r_m-1)})\\ &\quad + p(z, y_1, \cdots, y_1^{(r_1-1)}, \cdots, y_m^{(r_m-1)})u.\end{aligned} \quad (4.12)$$

If this transformation is possible, the ordered m-tuple $(r_1, r_2, \cdots, r_m)$ is called the vector relative degree. When we set the outputs $y_i \equiv 0$, we force all their derivatives and all u_i's to be equal to zero. The reduced order system

$$\dot{z} = f_0(z, 0, \cdots, 0) \quad (4.13)$$

obtained in this way is called *zero dynamics*. In the linear case this dynamics is completely determined by the system zeros. Using the linear analogy we say that a nonlinear system is minimum phase if its zero dynamics (4.13) is asymptotically stable. We say that a nonlinear system is nonminimum phase if its zero dynamics is unstable.

Returning to the diesel engine model (4.2), a natural choice of outputs for the input–output linearization is given by (4.6). However, this choice has a serious drawback that the corresponding zero dynamics given by (4.9) is unstable. This means that while $y_1 = y_2 = 0$ is maintained by the controls, the states of the zero dynamics may escape to infinity. Unstable zero dynamics presents an obstacle to control design using input–output linearization method [9], [21].

We circumvent this problem by redefining the outputs, replacing the relative degree 0 output $y_2 = W_{\mathrm{egr}} - W_{\mathrm{egr}}^d$ with the exhaust pressure

$$\bar{y} = \begin{bmatrix} \bar{y}_1 \\ \bar{y}_2 \end{bmatrix} := \begin{bmatrix} y_1 \\ p_2 - p_{2e} \end{bmatrix} \quad (4.14)$$

motivated by the fact that p_1 is the stable mode of the original zero dynamics while p_2 is the unstable one. By considering the exhaust pressure as an output, it ceases to be a part of the zero dynamics.

$$\begin{aligned}W_c^d &= \frac{W_f}{2}\Bigg[\mathrm{AF}_{ref}(1 - \mathrm{EGR}_{ref}) + 15.6\mathrm{EGR}_{ref} - 1\\ &\qquad + \sqrt{(\mathrm{AF}_{ref}(1 - \mathrm{EGR}_{ref}) + 15.6\mathrm{EGR}_{ref} - 1)^2 + 4(1 - \mathrm{EGR}_{ref})\mathrm{AF}_{ref}}\Bigg]\\ W_{\mathrm{egr}}^d &= \frac{\mathrm{EGR}_{ref}}{1 - \mathrm{EGR}_{ref}}\, W_c^d.\end{aligned} \quad (4.5)$$

A change of coordinates consistent with the chosen outputs gives

$$\begin{aligned}\dot{\overline{y}}_1 &= -a(\overline{y}_1 + W_c^d - k_e p_1) - \frac{1}{\tau}(\overline{y}_1 + W_c^d) - a v_1 + b v_2\\ \dot{\overline{y}}_2 &= k_2(k_e p_1 + W_f) - k_2 v_1 - k_2 v_2\\ \dot{p}_1 &= k_1(\overline{y}_1 + W_c^d - k_e p_1 + v_1).\end{aligned} \tag{4.15}$$

Because the determinant of the matrix

$$G := \begin{bmatrix} -a & b \\ -k_2 & -k_2 \end{bmatrix}$$

cannot vanish in Ω, we conclude that the relative degree is $(1, 1)$ and the corresponding zero dynamics is of dimension one. By solving for v_1 and v_2 that render $\overline{y} = \dot{\overline{y}} = 0$ and substituting this into the p_1 dynamics, we obtain a representation of the zero dynamics as

$$\dot{p}_1 = \frac{k_1(W_c^d + W_f)}{\tau k_1 \mu p_1^{\mu-1}(W_c^d + W_f) + p_{1e} - 1}(p_{1e}^\mu - p_1^\mu). \tag{4.16}$$

The function multiplying $(p_{1e}^\mu - p_1^\mu)$ is positive in Ω, and we conclude that the equilibrium p_{1e} of the zero dynamics is asymptotically stable.

With the zero dynamics stable, we can apply the standard stabilization technique for input–output linearizable systems. The feedback transformation

$$\begin{aligned}\begin{bmatrix} v_1 \\ v_2 \end{bmatrix} &= G^{-1}\\ &\times \left(\begin{bmatrix} w_1 \\ w_2 \end{bmatrix} - \begin{bmatrix} -a(\overline{y}_1 + W_c^d - k_e p_1) - \frac{1}{\tau}(\overline{y}_1 + W_c^d) \\ k_2(k_e p_1 + W_f) \end{bmatrix} \right)\end{aligned} \tag{4.17}$$

renders the system decoupled from the new inputs w_1 and w_2 to the outputs $\overline{y}_1$ and $\overline{y}_2$. After introducing a new coordinate $z := p_1^\mu - p_{1e}^\mu$ for the zero dynamics subsystem and some algebraic manipulations, we obtain the transformed system

$$\begin{aligned}\dot{\overline{y}}_1 &= w_1\\ \dot{\overline{y}}_2 &= w_2\\ \dot{z} &= q\Big[-W_c^d z + (d_1 - p_1^\mu + 1)\overline{y}_1\\ &\qquad + d_2 \overline{y}_2 - (p_1^\mu - 1)\tau w_1 - \frac{d_1}{k_2} w_2 \Big]\end{aligned} \tag{4.18}$$

where $q = (\mu p_1^{\mu-1} k_1)/(\tau(a+b)(p_1^\mu - 1))$, $d_1 = (p_1^\mu - 1)\tau b$, and $d_2 = \eta^*(T_2/T_a)(W_c^d + W_f)((p_{2e}^{-\mu} - p_2^{-\mu})/\overline{y}_2)$.

Now selecting $w_1 = -(1/\tau)\overline{y}_1$, $w_2 = -\alpha \overline{y}_2$, $\alpha > 0$, renders (4.18) a cascade of the stable nonlinear z-subsystem and the linear exponentially stable $\overline{y}$-subsystem. Note that $(p_1^\mu - 1)\overline{y}_1$ term in the z-dynamics is cancelled by our choice for w_1. Because q, d_1, and d_2 are bounded as functions of z, the cascade is globally (relative to Ω) asymptotically stable (cf. [22]). The system satisfies the conditions of [10] and a Lyapunov function can be constructed by adding a cross term $\Psi(z, \overline{y})$ to the sum

$$V = c_1 \overline{y}_1^2 + c_2 \overline{y}_2^2 + c_3 z^2. \tag{4.19}$$

Such a Lyapunov function becomes a CLF for the domination redesign.

However, computing Ψ in this case is difficult and leads to a complex Lyapunov function. Rather, we look for a possibility to make V (without Ψ) a CLF by an appropriate choice of c_1, c_2, and c_3. If this can be done, the simple form of the CLF guarantees that the final form of the domination redesign control law will be simple.

According to the definition, V is a CLF if $L_{\overline{g}_1} V = L_{\overline{g}_2} V = 0$ implies $L_{\overline{f}} V < 0$ for all $(\overline{y}_1, \overline{y}_2, z) \neq 0$, where $\overline{f}$, $\overline{g}_1$, and $\overline{g}_2$ correspond to the system (4.18). The conditions $L_{\overline{g}_1} V = L_{\overline{g}_2} V = 0$ become

$$\begin{aligned} L_{\overline{g}_1} V &= 2c_1 \overline{y}_1 - 2c_3(p_1^\mu - 1) q \tau z = 0\\ &\iff \overline{y}_1 = \frac{c_3}{c_1}(p_1^\mu - 1) q \tau z\\ L_{\overline{g}_2} V &= 2c_2 \overline{y}_2 - 2c_3 \frac{d_1}{k_2} q z = 0\\ &\iff \quad \overline{y}_2 = \frac{c_3 d_1}{c_2 k_2} q z. \end{aligned} \tag{4.20}$$

Substituting these into the expression for $L_{\overline{f}} V$ yields

$$\begin{aligned} L_{\overline{f}} V &= 2c_3 q z^2\\ &\quad \cdot \left[-W_c^d + (d_1 - p_1^\mu + 1)(p_1^\mu - 1) q \tau \frac{c_3}{c_1} + d_2 q \frac{c_3 d_1}{c_2 k_2} \right]. \end{aligned}$$

Obviously, $L_{\overline{f}} V < 0$ for $z \neq 0$ if the expression in brackets is negative in Ω. Using $q d_1 < k_1 \mu$, $(p_{2e}^{-\mu} - p_2^{-\mu})/\overline{y}_2 < \mu$, and the inequality $\eta^*(T_2/T_a)(p_1^\mu - 1) - (p_1^\mu - 1)^2 \leq (\eta^*(T_2/2T_a))^2$ we obtain a sufficient condition for V to be a CLF

$$\frac{1}{c_3} > \eta^* \frac{T_2}{T_a} \frac{\mu \tau k_1}{4 W_c^d} \frac{1}{c_1} + \eta^* \mu^2 \frac{T_1}{T_a} \frac{V_2}{V_1} \frac{W_c^d + W_f}{W_c^d} \frac{1}{c_2}. \tag{4.21}$$

This inequality can always be satisfied by selecting c_3 sufficiently small relative to c_1 and c_2. To illustrate how restrictive this condition is, we have assumed $T_{2,\max} = 1000K$, $T_{1,\max} = 450\text{K}$, $T_a = 300\text{K}$, $\tau = 0.15$, and $\eta^* = 0.5$. The upper bound on the term multiplying $1/c_2$, which is independent of the units, is 0.02. The term multiplying $1/c_1$ depends on the units; for p_1 in kPA, and W_c in g/s (so that their ranges are similar), its upper bound is about 0.05. We conclude that the condition (4.21) is not at all restrictive which means that c_1, c_2 and c_3 are relatively free to be tuned for the desired transient response when they become feedback gains in the domination redesign control law.

C. *Domination Redesign Control Law*

Having constructed the CLF V we employ it to obtain an inverse optimal control law with guaranteed robustness properties. Because V is a CLF for the system (4.18), it is a CLF for all systems that can be obtained from (4.18) by feedback, coordinate, and input transformations including the system (4.21). This system is rewritten here for the sake of convenience

$$\begin{aligned}\dot{\overline{y}}_1 &= -a(y_1 + W_c^d - k_e p_1) - \frac{1}{\tau}(\overline{y}_1 + W_c^d) - a v_1 + b v_2\\ \dot{\overline{y}}_2 &= k_2(k_e p_1 + W_f) - k_2 v_1 - k_2 v_2\\ \dot{p}_1 &= k_1(y_1 + W_c^d - k_e p_1 + v_1).\end{aligned} \tag{4.22}$$

Note that this is a form of the diesel engine model before we applied cancellations.

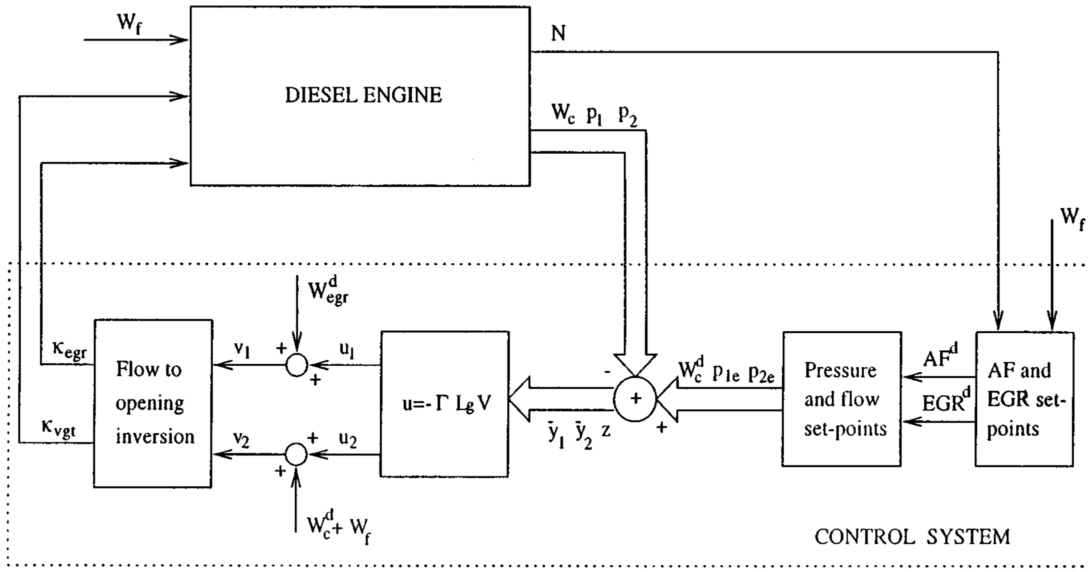

Fig. 3. Block diagram of the closed-loop system.

The domination redesign does not apply to v_1 and v_2 since $v_1 = v_2 = 0$ does not render the point $(0, 0, p_{1e})$ an equilibrium for (4.22). Hence, to proceed we center the controls at their set point values

$$u_1 := v_1 - W_{\text{egr}}^d, \qquad u_2 := v_2 - (W_c^d + W_f). \qquad (4.23)$$

Instead of computing $p_S(x)$ and dominate it with $\gamma(V)$, we choose $\gamma(\cdot) = \Gamma = \text{diag}\{\gamma_1, \gamma_2\}$ constant. As shown in Section III, this choice achieves semiglobal stability and provides an additional degree of freedom in tuning the control gains. Because V is quadratic and the Jacobian linearization of (4.18) is controllable we know that the stability and robustness to all $\Delta \in \mathcal{I}$ can be achieved on any compact set. Hence, the domination redesign control law takes the form as shown in (4.24). The stability and robustness of optimal systems are guaranteed provided that the feedback gains c_1, c_2, and c_3 satisfy the inequality (4.21) and γ_1, γ_2 are sufficiently large. With the final feedback control law given by (4.24), the block diagram of the closed-loop system that regulates AF ratio and EGR fraction to their desired set points is depicted in Fig. 3.

V. Simulation and Experimental Results

The performance of the controller given by (4.23) and (4.24) was evaluated in simulations and test-cell experiments. The simulation model is the seventh-order model of Section II augmented by the dynamics of the two actuators. It has been developed internally as reported in [15] and [26]. The drivers for the actuators are modeled as first-order (VGT) and second-order (EGR) linear systems. The maps for volumetric efficiency, engine temperature rise, and EGR mass flow rate were obtained from the static engine data. Isentropic efficiencies, turbine and compressor mass flow rates were determined from the maps provided by the manufacturer.

The design parameters γ_1, γ_2, c_1, c_2, and c_3, which actually provide only four degrees of freedom, are adjusted for best performance. Once calibrated, these parameters were held constant throughout the operating region.

In the implementation of the controller k_2 has been held constant. Further, to compute the set points for W_c, p_1, and p_2, simplified maps are used to evaluate k_e and T_2:

$$k_e = k_e(N), \qquad T_2 = T_2(\text{AF}^d)$$

while η^* has been held constant. Furthermore, nonlinear functions a and b have also been held constant to simplify the controller for implementation and avoid singularity when p_1 is equal to the ambient pressure. The latter problem, that cannot occur in the simulation model, is possible in a real engine. These simplifications have caused small discrepancies seen in Fig. 4 between the set points computed by the controller and the ones that would result in perfect regulation.

The plots correspond to the sequence of fueling changes from 2 to 6 kg/h and back at the fixed engine speed of 2000 r/min. The set point regulation of air-fuel ratio and EGR, depicted in the lowest two plots in Fig. 5, is quite accurate and, what is equally important, the air-fuel ratio response is fast indicating small turbo lag. The flat region in the AF plot at $\text{AF} = 18$ is caused by the fuel limiter often used in diesel engines to reduce particulate emissions.

$$\begin{bmatrix} u_1 \\ u_2 \end{bmatrix} = -\frac{1}{2}\Gamma(L_gV)^T = -\Gamma \begin{bmatrix} -c_1a(W_c - W_c^d) - c_2k_2(p_2 - p_{2e}) + c_3k_2\mu p_1^{\mu-1}(p_1^\mu - p_{1e}^\mu) \\ c_1b(W_c - W_c^d) - c_2k_2(p_2 - p_{2e}) \end{bmatrix}. \qquad (4.24)$$

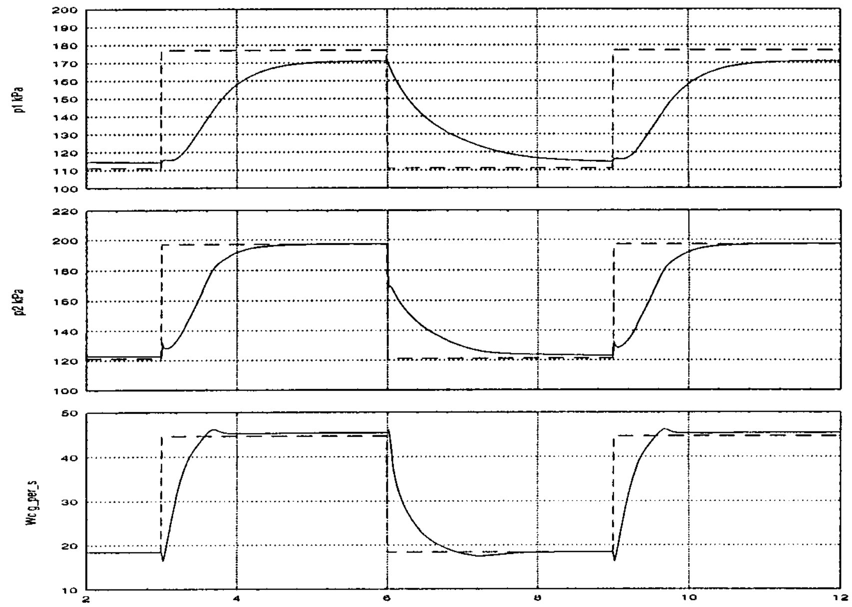

Fig. 4. Desired values (dashed) versus the actual values (solid) of the intake and exhaust manifold pressures and the compressor mass air flow rate.

Fig. 5. The commanded values (dash) versus the actual values (solid) of EGR and VGT openings, air-fuel ratio, and EGR flow fraction. The commanded values of EGR and VGT are generated by the control law while the commanded values for AF and EGR are from look-up tables.

The top two plots in Fig. 5 show the commanded values of the actuator openings $\kappa_{\rm egr}$ and $\kappa_{\rm vgt}$ (dash) and the actual openings of the actuators. The difference between them is due to the actuator dynamics. The performance of the closed-loop system indicates a degree of robustness of the control law, not only to weakly controllable/observable dynamics and parametric uncertainties, but also to the unmodeled dynamics of the actuators which changes the relative degree of the plant.

The controller has also been tested experimentally in a dynamometer test cell. Because the (in-cylinder) air-fuel ratio AF is not measured and has to be estimated dynamically from the measured data, we have decided to plot the exhaust air-fuel ratio instead. An advantage is that, in steady state, the exhaust air-fuel ratio is equal to W_c/W_f which is readily available from the measurements. Fig. 6 shows the exhaust air-fuel ratio and EGR set point regulation for the fueling step changes 3-5-7-5-3 kg/h at 2000 r/min.

The set points at 7 kg/h fuel rate are not feasible, but the transient performance is unaffected and the steady-state values of exhaust air-fuel ratio and EGR are acceptable.

The same set of feedback gains for the controller has been used at 3000 r/min for the same sequence of fueling. The traces

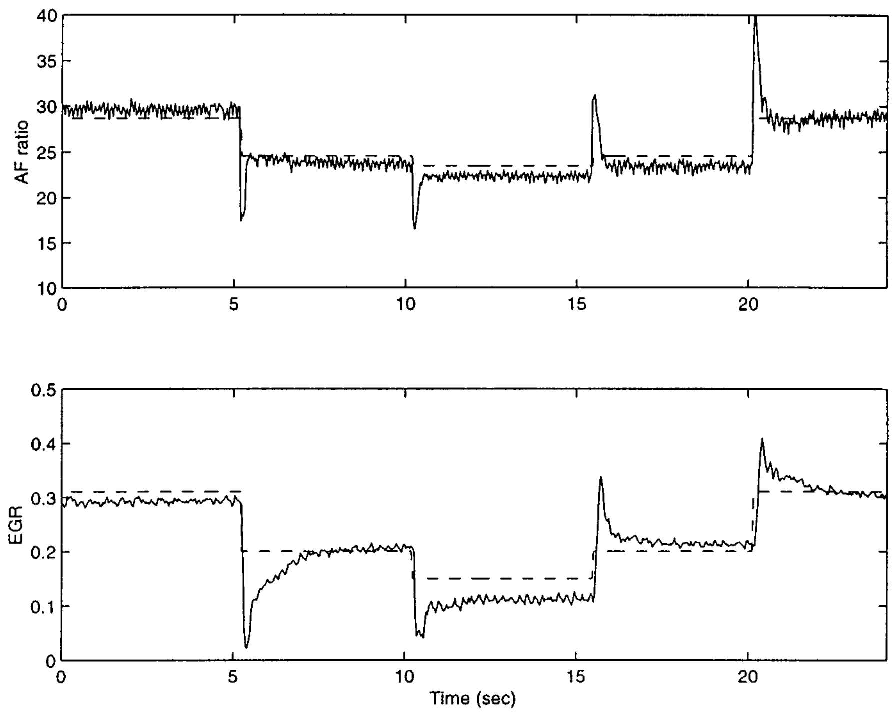

Fig. 6. Exhaust air-fuel ratio and EGR flow fraction set point regulation at 2000 r/min.

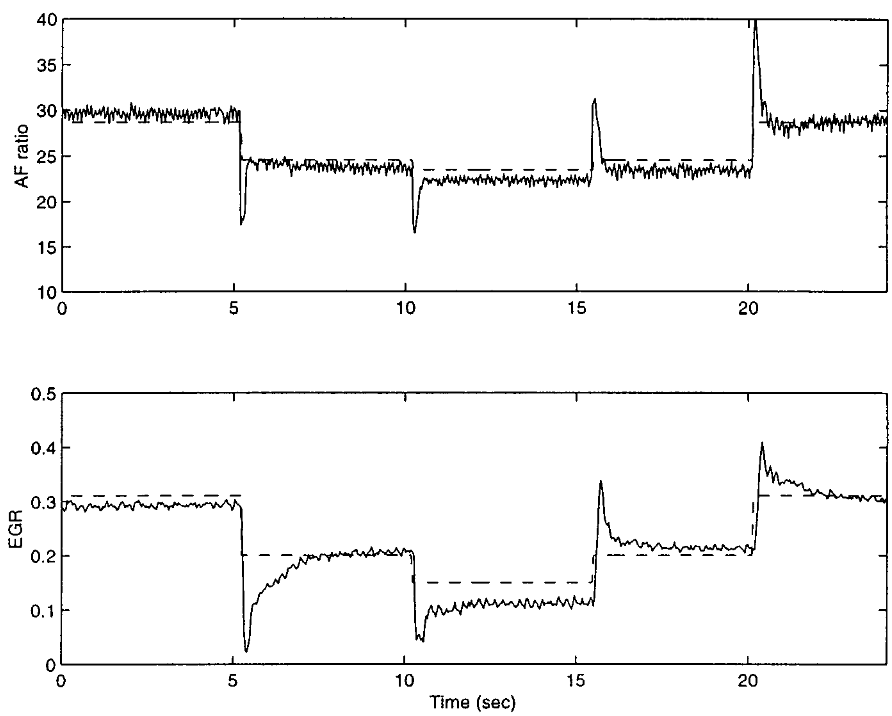

Fig. 7. Exhaust air-fuel ratio and EGR flow fraction set point regulation at 3000 r/min.

of exhaust air-fuel ratio and EGR regulation are shown in Fig. 7. It is interesting to compare these traces with the corresponding ones obtained at 2000 r/min. Obviously, steady-state values are different due to the higher engine pumping rate at higher speed. However, the transient responses of the AF ratio and EGR at the two engine speeds show remarkable similarity even though the same set of feedback gains has been used.

VI. Conclusion

In this paper we have presented an approach to design a controller for a turbocharged diesel engine. Interactions, nonlinearities and a significant level of uncertainty in the diesel engine model make this problem difficult. Our approach is based on a recently developed control design method which, starting from a CLF, provides a controller with a guaranteed robustness property interpretable as gain and phase margins. The required performance and simplicity desired for real-time automotive applications are achieved by judicious choice of the control design model and the CLF. A CLF is constructed by input–output linearization applied to the third-order model. Possible loss of robustness due to the cancellations used for the input–output linearizing control has been avoided because our final control law depends only on the CLF and not on the intermediate feedback transformations used in constructing it. The performance of the controller has been illustrated in simulations and experiments.

ACKNOWLEDGMENT

The authors would like to thank J. Cook, P. Moraal, and A. Stefanopoulou, for fruitful discussions and help, M. van Nieuwstadt for setting up the experimental facilities and substantial help in obtaining experimental results, and B. Powell for the support given to the second author during the course of this research.

REFERENCES

[1] B. D. O. Anderson and J. B. Moore, *Optimal Control: Linear Quadratic Methods*. Englewood Cliffs, NJ: Prentice-Hall, 1990.

[2] A. Amstutz and L. R. Del Re, "EGO sensor based robust output control of EGR in diesel engines," *IEEE Trans. Contr. Syst. Technol.*, vol. 3, pp. 39–48, Mar. 1995.

[3] Z. Artstein, "Stabilization with relaxed controls," *Nonlinear Anal.*, vol. 7, pp. 1163–1173, 1983.

[4] H. J. Dekker and W. L. Sturm, "Simulation control of a HD diesel engine equipped with new EGR technology," in SAE, 1996, paper 960 871.

[5] R. A. Freeman and P. V. Kokotović, *Robust Control of Nonlinear Systems*. Boston, MA: Birkhauser, 1996.

[6] S. T. Glad, "Robustness of nonlinear state feedback—A survey," *Automatica*, vol. 23, pp. 425–435, 1987.

[7] J. W. Grizzle, J. A. Cook, and W. P. Milam, "Improved air charge estimation for transient air fuel ratio control," presented at the Proc. of American Control Conference, Baltimore, MD, 1994, Paper TM01-1:30.

[8] E. Hendricks, A. Chevalier, M. Jensen, S. C. Sorensen, D. Trumpy, and J. Asik, "Modeling of the intake manifold filling dynamics," in SAE, 1996, paper 960 037.

[9] A. Isidori, *Nonlinear Control Systems*, 2nd ed. Berlin, Germany: Springer Verlag, 1989.

[10] M. Jankovic, R. Sepulchre, and P. V. Kokotović, "Constructive Lyapunov stabilization of nonlinear cascade systems," *IEEE Trans. Automat. Contr.*, pp. 1723–1753, 1996.

[11] ——, "CLF-based designs with robustness to dynamic input uncertainties," *Syst. Contr. Lett.*, vol. 37, pp. 45–54, 1999.

[12] J. P. Jensen, A. F. Kristensen, S. C. Sorenson, N. Houbak, and E. Hendricks, "Mean value modeling of a small turbocharged diesel engine," in SAE, 1991, paper 910 070.

[13] R. E. Kalman, "When is a linear control system optimal?," *Trans. ASME Ser. D: J. Basic Eng.*, vol. 86, pp. 1–10, 1964.

[14] M. Kao and J. J. Moskwa, "Turbocharged diesel engine modeling for nonlinear engine control and state estimation," *ASME J. Dynamic Syst., Measurement, Contr.*, 1995.

[15] I. Kolmanovsky, P. Moraal, M. van Nieuwstadt, and A. Stefanopoulou, "Issues in modeling and control of intake flow in variable geometry turbocharged engines," in *Proc. 18th IFIP Conf. Syst. Modeling Optimization*, Detroit, MI, July 1997.

[16] M. Krstić, I. Kanellakopoulos, and P. V. Kokotović, *Nonlinear and Adaptive Control Design*. New York: Wiley, 1995.

[17] R. Marino and P. Tomei, *Nonlinear Control Design*. Englewood Cliffs, NJ: Prentice-Hall, 1995.

[18] J. Moody, "Variable geometry turbocharging with electronic control," in SAE, 1986, paper 860 107.

[19] P. J. Moylan, "Implications of passivity in a class of nonlinear systems," *IEEE Trans. Automat. Contr.*, vol. 19, pp. 373–381, 1974.

[20] P. J. Moylan and B. D. O. Anderson, "Nonlinear regulator theory and an inverse optimal control problem," *IEEE Trans. Automat. Contr.*, vol. 18, pp. 460–465, 1973.

[21] H. Nijmeijer and A. van der Schaft, *Nonlinear Dynamical Control Systems*. New York: Springer-Verlag, 1990.

[22] R. Sepulchre, M. Jankovic, and P. V. Kokotović, *Constructive Nonlinear Control*. London, U.K.: Springer-Verlag, 1997.

[23] E. D. Sontag, "A universal construction of Artstein's theorem on nonlinear stabilization," *Syst. Contr. Lett.*, vol. 13, pp. 117–123, 1989.

[24] R. Stone, *Introduction to Internal Combustion Engines*, 2nd ed. Warendale, PA: SAE International, 1992.

[25] J. N. Tsitsiklis and M. Athans, "Guaranteed robustness properties of multivariable nonlinear stochastic optimal regulators," *IEEE Trans. Automat. Contr.*, vol. 29, pp. 690–696, 1984.

[26] M. van Nieuwstadt, P. E. Moraal, I. V. Kolmanovsky, A. Stefanopoulou, P. Wood, and M. Criddle, "Decentralized and multivariable design for EGR-VGT control of a diesel engine," in *Proc. IFAC Wkshp. Advances Automotive Contr.*, Mohican State Park, OH, 1998.

[27] N. Watson and M. Marzouk, "A nonlinear digital simulation of turbocharged diesel engines under transient conditions," in SAE, 1977, paper 770 123.

Mrdjan Jankovic (M'94–SM'99) received the B.S. degree from the University of Belgrade, Yugoslavia, in 1986, the M.S. and D.Sc. degrees from Washington University, St. Louis, MO, in 1989 and 1992.

He held postdoctoral teaching and research positions with Washington University and the University of California at Santa Barbara. He joined Ford Research Laboratories in 1995, where he currently holds a Senior Technical Specialist position working on the development of advanced powertrain control systems. His research interests include nonlinear estimation, nonlinear control, adaptive control, and control applications to automotive systems. He has coauthored numerous technical papers and one book.

Dr. Jankovic has served as an Associate Editor for IEEE TRANSACTIONS ON CONTROL SYSTEMS TECHNOLOGY since 1997.

Miroslava Jankovic received the B.S. degree from the University of Belgrade, Yugoslavia, in 1987, and the M.S. and D. Sc. degrees from Washington University, St. Louis, MO, in 1990 and 1994, respectively.

Since 1996, she has been with Ford Research Laboratory, where she works on the development of models and control algorithms for various hybrid electric vehicle drivetrain components.

Ilya Kolmanovsky (S'94–M'95) received the M.S. degrees in mathematics and aerospace engineering in 1993 and the Ph.D. degree in aerospace engineering in 1995 from the University of Michigan, Ann Arbor.

He is presently a technical Specialist with Ford Research Laboratory in Dearborn, MI, conducting research on advanced powertrain modeling and control.